Study on the Performance of Finely Ground Recycled Concretes in Cementitious Pastes

Václav Nežerka, Zdeněk Prošek, and Radim Hlůžek
Faculty of Civil Engineering, Czech Technical University in Prague, Thákurova 7, 166 29 Praha 6, Czech Republic
Email: {vaclav.nezerka, zdenek.prosek, radim.hluzek}@fsv.cvut.cz

***Abstract*—Mobile grinders could be used for instant recycling of concrete waste, eliminating the need for transport of the demolition waste, storing, and possibly also landfilling. Even though partial replacement of aggregate by recycled one has become established practice, incorporation of concrete fines composed of fine sand and stripped mortar into concrete mix has been considered harmful. However, these fines could contribute to the concrete matrix and ITZ strengthening by the microfilling effect and through activation of residual anhydrous clinker (RAC). This study focuses on the content and possible reactivation of RAC from various sources in cementitious pastes using microscopy, calorimetry, and macroscopic testing of mechanical properties. The results indicate that proper sorting of the recycled material before grinding is crucial.**

***Index Terms*—demolition waste, recycled concrete, residual anhydrous clinker, mechanical properties, grinding**

I. Introduction

The incorporation of demolition waste into concrete mixes represents a cheap solution to tackle the environmental burden of landfilling [1] and emissions related to the Portland cement production [2, 3]. Use of mobile grinders in the demolition sites would bring both ecological and economic benefits.

A partial replacement of aggregates by recycled ones has become a common practice in the construction industry and the inconveniences connected to their use of, such as altered workability, lower strength, and deteriorated durability [4, 5], have been overcome [6]. However, utilization of fine fractions is restricted or even forbidden [7] due to their impact on concrete performance. Recent findings [4, 8] indicate that the incorporation of recycled concrete fines (RCF) after careful design of the concrete mix.

It was reported that incorporation of RCF can enhance performance of cement pastes if blended with fly ash or blast furnace slag [9]. These improvements were attributed to filling of voids by RCF particles, their beneficial effect on cement hydration, and reactivation of RAC. The presented study is focused on the effect of type, age, origin, and sorting of recycled concrete on the presence of RAC and behavior of cementitious pastes containing RCF.

Manuscript received July 7, 2019; revised May 11, 2020.

II. Materials

A. Recycled Concrete

Four types of recycled concrete (Table I) were prepared. First RCF material, prestressed recycled railway sleeper (RRS), was prepared from high-quality concrete (class C44/55 [10]). The sleeper was used in a railway track and subjected to weathering. Next, RCF from a recycled drainage channel (RDC) was prepared from a precast unit. Finally, recycled reinforced concrete from monolithic columns was selected as a third material for production of RCF. All RCF materials were produced by crushing of recycled concrete to a 0–16 mm particle size, separation of rebars, and grinding. In the case of recycled concrete from old columns, crushed concrete was split to two samples: in the first one (RC1) only the 0–1 mm fraction was separated for grinding so that it contained stripped mortar with a low amount of aggregates, while the other sample (RC2) was ground with aggregates, as in the case of RRS and RDC.

Individual RCF types were blended with ordinary Portland cement (PC) CEM I/42.5R, to produce cementitious pastes. The particle size distribution of PC and RCF is presented in Fig. 1.

TABLE I. Summary of Recycled Concrete Materials

Material	Description		
	Origin	Age	Recycling
RRS	Railway sleeper	50 years	Crushing, grinding
RDC	Drainage channel	4 years	Crushing, grinding
RC1	Building column	107 years	Crushing, extraction of fines, grinding
RC2	Building column	107 years	Crushing, grinding

B. Tested Materials and Samples

The studied cementitious pastes (Table II) were produced by blending PC with RCF using an electric blender. Water to binder ratio, w/b, was equal to 0.35 in all pastes. The pastes were cast into 40×40×160 mm prismatic molds, compacted using a shaking table, and removed from molds after 24 hours. Hardening took place in the laboratory at 22◦C and 100% relative

© 2020 Int. J. Struct. Civ. Eng. Res.
doi: 10.18178/ijscer.9.3.269-272

humidity for 28 days. Six prismatic specimens represented each mix.

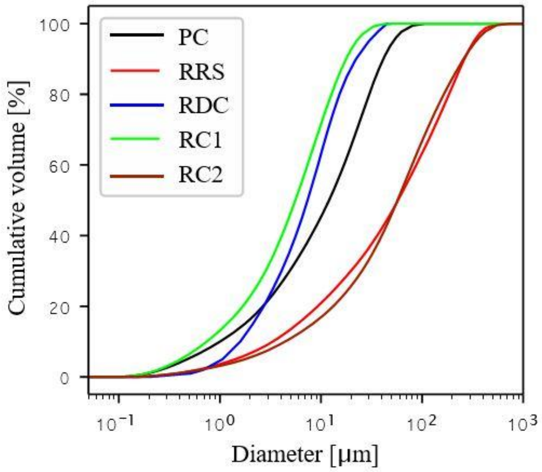

Figure 1. Particle size distribution curves of input materials.

TABLE II. COMPOSITION OF THE PREPARED MIXES (WT.%)

Mix	PC	RRS	RDC	RC1	RC2	*w/b*
R	100	-	-	-	-	
RS-10	90	10	-	-	-	
RS-20	80	20	-	-	-	
RS-30	70	30	-	-	-	
RS-40	60	40	-	-	-	
RS-50	50	50	-	-	-	
DG-10	90	-	10	-	-	
DG-20	80	-	20	-	-	
DG-30	70	-	30	-	-	
DG-40	60	-	40	-	-	
DG-50	50	-	50	-	-	0.35
C1-10	90	-	-	10	-	
C1-20	80	-	-	20	-	
C1-30	70	-	-	30	-	
C1-40	60	-	-	40	-	
C1-50	50	-	-	50	-	
C2-10	90	-	-	-	10	
C2-20	80	-	-	-	20	
C2-30	70	-	-	-	30	
C2-40	60	-	-	-	40	
C2-50	50	-	-	-	50	

III. EXPERIMENTAL METHODS

A. SEM-BSE

SEM-BSE analysis was carried out using a FEG-SEM Merlin ZEISS scanning electron microscope to investigate morphology and distribution of individual phases. Mapping of microstructure was carried out at a 1000× magnification on a total area of 4.2 mm^2 using a PyPAIS software [11].

B. Calorimetry

An eight-channel isothermal heat flow calorimeter TAM Air, manufactured by Thermometric AB Sweden, was used to detect all hydration stages during the first 5 days of hardening. The generated heat was normalized to 1 g of PC in the mix in order to reveal the contribution of individual RCF.

C. Testing of Stiffness and Strength

The dynamic Young's modulus of pastes was determined non-destructively using the resonance method [12], based on a measurement of longitudinal vibration of specimens [13].

Tensile strength in bending was determined from a three-point bending test and a uniaxial compression test was carried out on portions of beams broken in the bending test. A 10 mm thick steel plate was used to ensure a uniform stress distribution over a 40×40 mm area.

IV. RESULTS AND DISCUSSION

A. Microstructure

SEM-BSE images were used for segmentation and assessment of individual phases (Fig. 2). It revealed that coarser RCF contained RAC embedded within hydrated cementitious matrix. Disintegration of these matrix fragments in RC1 allowed better access of water to RAC and promoted RAC hydration, as observed during calorimetry measurements.

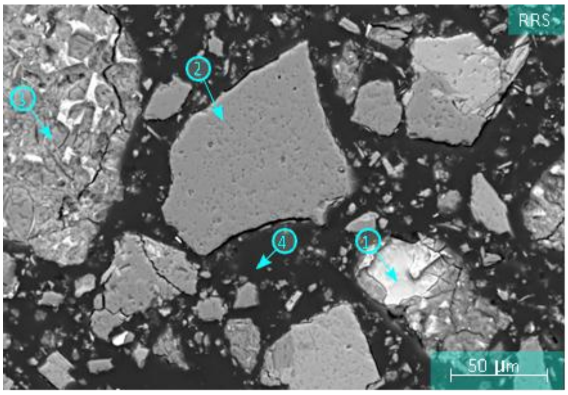

Figure 2. Microscopy image at 1000× magnification of RRS embedded in epoxy resin with markers denoting (1) RAC, (2) fragments of aggregates, (3) fragments of hydrated cementitious matrix, and (4) epoxy resin.

TABLE III. RESULTS OF IMAGE ANALYSIS OF PHASES FROM SEM-BSE IMAGES

	Volume fraction [%]		
RCF	RAC	Paste	Aggregates
RRS	4.91±0.41	12.94±3.52	81.93±7.32
RDC	1.97±0.35	33.32±10.32	63.71±10.52
RC1	8.49±0.55	42.36±8.34	49.15±8.85
RC2	3.19±0.48	34.40±11.33	62.41±10.82

B. Hydration Heat

Specific heat flow and cumulative hydration heat were measured to identify hydration stages and evaluate the total heat released during the first 5 days of hydration, see Fig. 3.

© 2020 Int. J. Struct. Civ. Eng. Res.

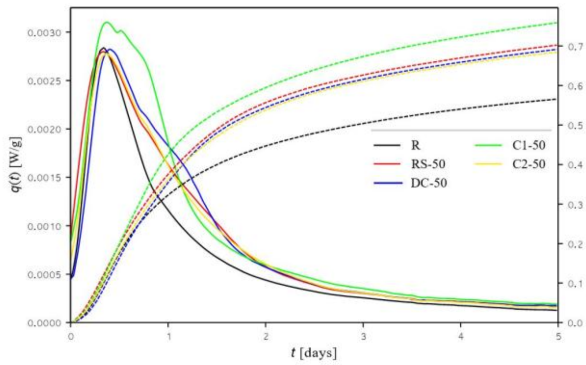

Figure 3. Specific heat flow q(t) (solid lines) and cumulative hydration heat *Q(t)* (dashed lines) released during the first 5 days of hydration, normalized to 1 g of PC in the mix.

The secondary bump within the deceleratory period at around first day of hydration in the pastes containing RCF can be attributed to a transformation of ettringite to monosulphate. The separation of fines during production of RC1 resulted in an increase of *q(t)* peak during hydration of the C1-50 paste. This peak can be attributed to the hydration of C3S and formation of low-density C-S-H gel.

TABLE IV. TOTAL AMOUNT OF HEAT PRODUCED DURING FIRST 5 DAYS OF HYDRATION, NORMALIZED TO 1 G OF PC IN THE MIX

	R	RS-50	DC-50	C1-50	C2-50
Q_5 [kJ/g]	0.565	0.702	0.691	0.759	0.684

C. Mechanical Properties

It is obvious from Figs. 4 and 5 that the addition of larger amounts of RCF is responsible for deterioration of stiffness and strength, however, this deterioration is not significant. This deterioration is lowest in the case of RC1, which is in contradiction with the porosity measurement. It can be conjectured that the fine grinding of RC1 and higher amount of RAC increase the integrity of the cementitious matrix.

On the other hand, the lack of larger particles seems disadvantageous when the paste specimens are subjected to tensile stresses. Larger grains of RC2 act partially as aggregate reinforcing the brittle matrix, see Fig. 6.

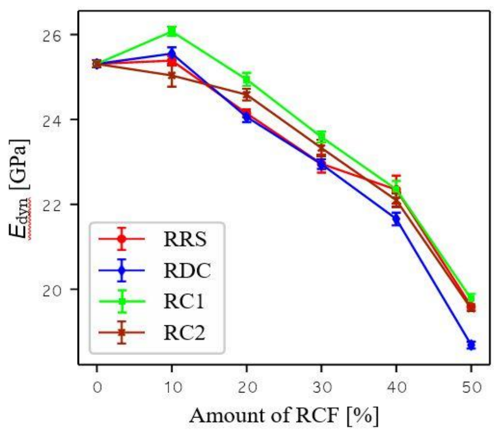

Figure 4. Impact of individual RCF on stiffness of pastes after 28 days of hardening.

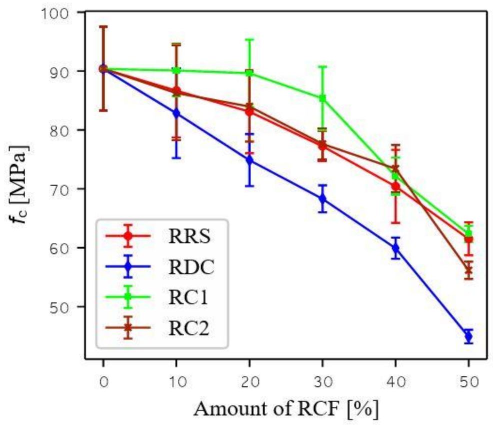

Figure 5. Impact of individual RCF on compressive strength of pastes after 28 days of hardening.

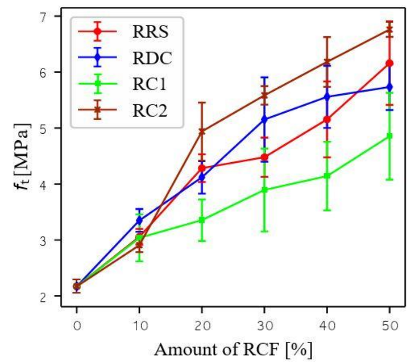

Figure 6. Impact of individual RCF on tensile strength of pastes after 28 days of hardening.

V. CONCLUSIONS

The study revealed that RCF can be incorporated in rather large amounts in cementitious composites without sacrificing their structural performance. As shown by calorimetry measurements, RCF containing the highest amount of RAC generated highest amount of heat during the first 5 days of hydration, when normalized to 1 g of PC in the mix. Therefore, it can be conjectured that the presence of RCF promotes hydration and some portion of RAC in RCF could be reactivated. This reactivation can be responsible for the compact matrix of specimens containing RCF rich in RAC. This was reflected by a very limited deterioration of compressive strength in samples where the amount of detected clinker was largest. The positive impact of RCF on bending strength can be rather attributed to bridging of microcracks and increase of fracture energy.

CONFLICT OF INTEREST

The authors declare no conflict of interest.

AUTHOR CONTRIBUTIONS

All authors participated in the experimental activities. V. Nežerka and R. Hlůžek analyzed the data, Z. Prošek designed the experiments, and V. Nežerka wrote the paper. All authors had approved the final version.

ACKNOWLEDGMENT

This work was supported by the Czech Science Foundation [grant number GA ČR 17-06771S] and the Faculty of Civil Engineering at CTU in Prague [grant number SGS20/037/OHK1/1T/11].

REFERENCES

[1] D. Gastaldi, F. Canonico, L. Capelli, L. Buzzi, E. Boccaleri, S. Irico, "An investigation on the recycling of hydrated cement from concrete demolition waste," *Cement and Concrete Composites*, vol. 61, pp. 29–35, 2015.

[2] US Geological Survey & Orienteering S and US Geological Survey, Mineral Commodity Summaries, 2009, Government Printing Office, 2009.

[3] J. M. Paris, J. G. Roessler, C. C. Ferraro, H. D. DeFord, T. G. Townsend, "A review of waste products utilized as supplements to portland cement in concrete," *Journal of Cleaner Production*, vol. 121, 2016, pp. 1–18.

[4] L. Evangelista, J. de Brito, "Durability performance of concrete made with fine recycled con- crete aggregates," *Cement and Concrete Composites*, vol. 32, pp. 9–14, 2010.

[5] D. Pedro, J. de Brito, L. Evangelista, "Durability performance of high-performance concrete made with recycled aggregates, fly ash and densified silica fume," *Cement and Concrete Composites*, vol. 93, pp. 63–74, 2018.

[6] M. Thiery, P. Dangla, P. Belin, G. Habert, N. Roussel, "Carbonation kinetics of a bed of recycled concrete aggregates: A laboratory study on model materials," *Cement and Concrete Research*, vol. 46, pp. 50–65, 2013.

[7] L. Evangelista, J. De Brito, "Durability of crushed fine recycled aggregate concrete assessed by permeability-related properties," *Magazine of Concrete Research*, 2018.

[8] J. Khatib, "Properties of concrete incorporating fine recycled aggregate," *Cement and Concrete Research*, vol. 35, pp. 763–769, 2005.

[9] Z. Prošek, V. Nežerka, R. Hlůžek, J. Trejbal, P. Tesárek, G. Karra ́a, "Role of lime, fly ash, and slag in cement pastes containing recycled concrete fines," *Construction and Building Materials*, vol. 201, pp. 702–714, 2019.

[10] Eurocode 2. design of concrete structures, doi:10.3403/30096437.

[11] V. Nežerka and J. Trejbal, 2019, "Assessment of aggregate-bitumen coverage using entropy-based image segmentation," *Road Materials and Pavement Design*.

[12] ASTM International, Test Method for Dynamic Youngs Modulus, Shear Modulus, and Pois- sons Ratio by Impulse Excitation of Vibration, 2006. doi:10.1520/e1876-01r06.

[13] V. Nežerka, Z. Slížková, P. Tesárek, T. Plachý, D. Frankeová, V. Petráňová, "Comprehensive study on microstructure and mechanical properties of lime-pozzolan pastes," *Cement and Concrete Research*, vol. 64, 2014, pp. 17–29.

Copyright © 2020 by the authors. This is an open access article distributed under the Creative Commons Attribution License (CC BY-NC-ND 4.0), which permits use, distribution and reproduction in any medium, provided that the article is properly cited, the use is non-commercial and no modifications or adaptations are made.